

# Aerosol Spectra and New Particle Formation Observed in Various Seasons in Nanjing

ZHU Bin\* (朱彬), WANG Honglei (王红磊), SHEN Lijuan (沈利娟),  
KANG Hanqing (康汉青), and YU Xingna (于兴娜)

*Key Laboratory of Meteorological Disaster of Ministry of Education, Nanjing  
University of Information Science and Technology, Nanjing 210044*

(Received 22 August 2012; revised 16 January 2013; accepted 21 January 2013)

## ABSTRACT

The aerosol number spectrum and gas pollutants were measured and the new particle formation (NPF) events were discussed in Nanjing. The results showed that the size distributions of aerosol number concentrations exhibited distinct seasonal variations, implying the relations of particle sizes and their sources and sinks. The number concentrations of particles in the nuclei mode (10–30 nm), Aitken mode (30–100 nm), accumulation mode (100–1000 nm) and coarse mode ( $>1 \mu\text{m}$ ) varied in the order of summer  $>$  spring  $>$  autumn, summer  $>$  autumn  $>$  spring, autumn  $>$  summer  $>$  spring, and spring  $>$  autumn  $>$  summer, respectively. The diurnal variation of total aerosol number concentrations showed three peaks in all observed periods, which corresponded to two rush hours and the photochemistry period at noon. In general, the NPF in summer occurred under the conditions of east winds and dominant air masses originating from marine areas with high relative humidity (50%–70%) and strong solar radiations ( $400\text{--}700 \text{ W m}^{-2}$ ). In spring, the NPF were generally accompanied by low relative humidity (14%–30%) and strong solar radiations ( $400\text{--}600 \text{ W m}^{-2}$ ). The new particle growth rates (GR) were higher in the summertime in the range of  $10\text{--}16 \text{ nm h}^{-1}$ . In spring, the GR were  $6.8\text{--}8.3 \text{ nm h}^{-1}$ . Under polluted air conditions, NPF events were seldom captured in autumn in Nanjing. During NPF periods, positive correlations between 10–30 nm particles and  $\text{O}_3$  were detected, particularly in spring, indicating that NPF can be attributed to photochemical reactions.

**Key words:** atmospheric aerosol, size spectrum, new particle formation, trace gases

**Citation:** Zhu, B., H.-L. Wang, L.-J. Shen, H.-Q. Kang, and X.-N. Yu, 2013: Aerosol spectra and new particle formation observed in various seasons in Nanjing. *Adv. Atmos. Sci.*, **30**(6), 1632–1644, doi: 10.1007/s00376-013-2202-4.

## 1. Introduction

Atmospheric aerosols are the primary pollutants leading to the deterioration of urban air quality (Horvath et al., 1996), which result in frequent haze events and declining visibility in urban and regional scales (Jung and Kim, 2006). Epidemiological studies have shown that these atmospheric particles, particularly those of ultrafine composition, endanger human health and lead to respiratory diseases (Natusch and Wallace, 1974; Donaldson et al., 2002). Studies have shown that the climate and health effects of atmospheric aerosols are strongly related to their size distributions, chemical compositions, and mixing states (Holmes, 2007; Li et al., 2010). Aerosol size distributions exhibit obvi-

ous seasonal variations and are significantly affected by meteorological factors (Wehner and Wiedensohler, 2003; Catro et al., 2010). Moreover, researchers have determined that the aerosol number concentrations and size distributions are controlled by local sources and physical and chemical processes of aerosols and are diverse in various functional areas of urban atmospheres including downtown, suburban, and scenic areas in addition to regions along highways (McMurry and Woo, 2002; Wehner et al., 2002; Putaud et al., 2010).

These size distributions and chemical compositions of aerosols may indicate their residence times and source/sink information. Therefore, aerosol sources could be identified by analyzing their number spec-

\*Corresponding author: ZHU Bin, binzhu@nuist.edu.cn

tra and chemical compositions. For example, particles in the nuclei mode (10–30 nm) are formed mainly from atmospheric nucleation events related to gas-to-particle transformation and growth of nanometer-scale particles. Aitken mode particles (30–100 nm) could be emitted directly from combustion sources such as vehicle emissions and may also result from the condensation and coagulation of nuclei mode particles. Accumulation mode particles (100–1000 nm) originate from condensation and coagulation of Aitken mode particles. Coarse particles (>1  $\mu\text{m}$ ) are formed by mechanical processes and generally consist of anthropogenic and natural dust (Kulmala et al., 2004a).

New particle formation (NPF) events could occur widely in a regional scale under various meteorological and atmospheric environmental conditions worldwide (Kulmala et al., 2004a, b; Dal Maso et al., 2005; Hussein et al., 2009; Gong et al., 2011). Previous NPF observation studies were centralized mainly in clean environments (Mäkelä et al., 1997; Dal Maso et al., 2005; Hussein et al., 2009). Moreover, NPF events have recently been studied in some cities of developed countries (Jeong et al., 2004; Kuang et al., 2009) and in some megacities of developing countries such as Mexico, New Delhi, and Beijing (Dunn et al., 2004; Wehner et al., 2004; Mönkkönen et al., 2005; Wu et al., 2007). Related studies indicate that sulfuric acid plays a dominant role in the NPF and the growth of particles (Boy et al., 2005; Riipinen et al., 2007), and positive correlations have been reported between the new particle nucleation rates and sulfuric acid levels. Organic compounds have also been considered as significant contributors to NPF, particularly when coexisting with sulfuric acid (Odum et al., 1997; Zhang et al., 2004). These studies demonstrated that the NPF-forming conditions are more complex in urban areas than those in clean areas. Therefore, additional observations are needed to reveal the methods by which particles form and grow in polluted urban environments.

Rapid urbanization and industrialization significantly influence the physical and chemical characteristics of aerosols. The Yangtze River Delta is one of the fastest developing economic regions in East Asia and includes the city of Nanjing, which is an important comprehensive industrial production base and transport hub. Nanjing's air pollution has worsened in recent years, leading to an increased number of haze days and fine-particle number concentration events. Aerosol particles are currently considered one of the most harmful air pollutants in this city (Qian et al., 2008). However, few systematic studies of the NPF have been conducted in Nanjing until recently. In this paper, therefore, the aerosol number spectra and trace gases were observed during three periods includ-

ing 19 October–27 November 2009; July 2010; and April–May 2011 in Nanjing. Moreover, the seasonal variations of aerosol number concentration and aerosol spectra are analyzed, and NPF events and related formation conditions are discussed.

## 2. Instruments and experiments

### 2.1 Sites and experiment descriptions

Two sites were selected in the downtown and suburban areas of Nanjing. The downtown site is located at the Drum Tower Campus of Nanjing University (DTNJ) (32.06°N, 118.78°E), which represents residential and business areas. No local emission sources are located within 200 m surrounding DTNJ. The second site is located at the campus of the Nanjing Information Engineering University (NUIST) (32.21°N, 118.72°E) in the northern suburb of Nanjing, approximately 3 km southwest of the Nanjing Chemical Industry area. No local emission sources are located within a radius of 500 m from the site, which includes a highway to east located approximately at the range boundary. This region represents a combination of traffic, industry, and cropland. The straight-line distance between the two sites is approximately 13 km. Under the same synoptic system, the air pollutants displayed similar features (Li et al., 2011). Observations were conducted during three periods of 19 October–24 November 2009; 9–28 July 2010; and 6 April–8 May 2011. The locations of the sites are shown in Fig. 1, and details of the observations are listed in Table 1.

### 2.2 Observational instruments

Particle number concentrations within 10 nm–10  $\mu\text{m}$  were measured by the Wide Range Particle Spectrometer (WPS) produced by MSP Corporation (USA). Details of this instrument were reported by Gao et al. (2009). Invalid data including RH of >90% and temperature ( $T$ ) of >35 °C were not included in the following analysis because the credible working conditions of WPS are RH 0%–90% and  $T < 35^\circ\text{C}$ . Theoretically, WPS has no detection limit. The concentration has  $a \pm 10\%$  error as indicated by the manufacturer.

Trace gases detected at NUIST were measured by Differential Optical Absorption Spectroscopy (DOAS), AR500 system, produced by OPSIS AB (Sweden; Opsis, 2003). The detection limits of  $\text{O}_3$ ,  $\text{NO}_2$ , and  $\text{SO}_2$  were 1  $\mu\text{g m}^{-3}$ , 0.3  $\mu\text{g m}^{-3}$ , and 0.3  $\mu\text{g m}^{-3}$ , respectively, and the zero drift was  $\pm 2 \mu\text{g m}^{-3}$ ,  $\pm 0.6 \mu\text{g m}^{-3}$ , and  $\pm 0.6 \mu\text{g m}^{-3}$ , respectively. Trace gases observation at DTNJ was conducted by emission monitoring systems (EMS) produced by Thermo Fisher Scientific that included the Thermo Electron model 42i chemi-

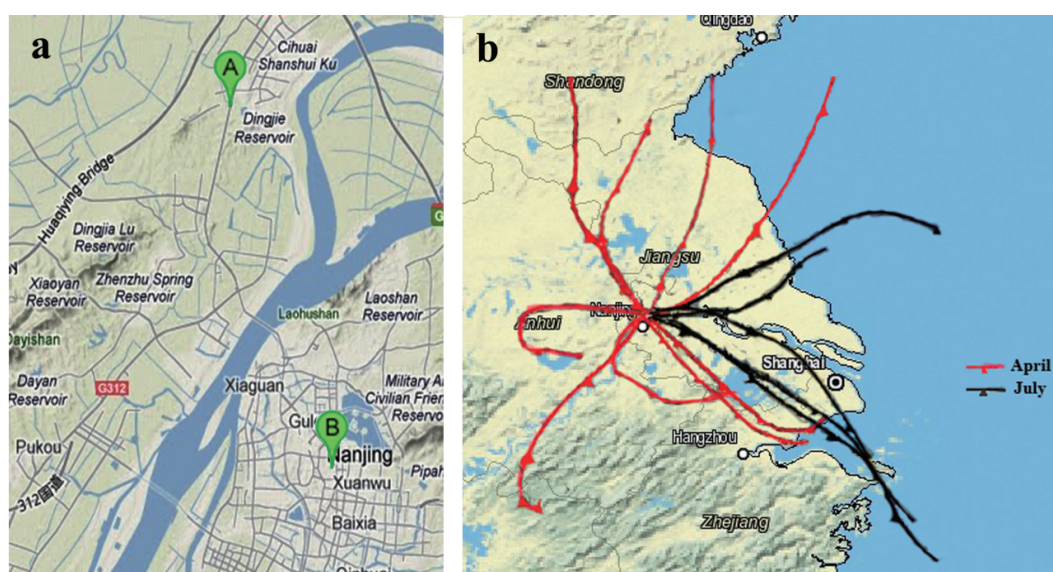


**Fig. 1.** The coarse resolution map show Nanjing and its surrounding regions, and the 24-h back trajectories of the air masses ending at 100-m height of Nanjing, in the periods of New Particle Formation (NPF). The fine resolution map in the upper-left indicates the two observational sites of this study (A: NUIST; B: DTNJ).

**Table 1.** The instruments, observation periods and sample amounts at the observation sites.

Instrument	Location	Observation time (samples numbers)
WPS	NUIST (above ground 36m)	19 Oct–1 Nov 2009 (3440); 9 Jul–28 Jul 2010 (4440)
	DTNJ(above ground 6m)	2 Nov–24 Nov 2009 (4223); 6 Apr–8 May 2011 (7746)
DOAS	NUIST(above ground 36m)	19 Oct–1 Nov 2009 (3768); 9 Jul–28 Jul 2010 (5760)
EMS	DTNJ(above ground 6m)	19 Oct–27 Nov 2009 (5142); 6 Apr–29 Apr 2011 (6226)

luminescent NO–NO<sub>2</sub>–NO<sub>x</sub> analyzer, the TEI model 49i ultraviolet (UV) light-emitting O<sub>3</sub> analyzer, and the TEI model 43i pulsed fluorescence SO<sub>2</sub> analyzer. A comparison of the two datasets of these gasses measured simultaneously by the two instrument systems is shown in Li et al. (2011).

Meteorological factors including wind speed/direction, temperature, pressure, relative humidity, radiation, and precipitation were obtained from the automatic weather station CSI-CR1000.

In this study, only one WPS was used to alternately measure the aerosol number spectra at the two sites. For the seasonal comparison, the data were obtained solely at DTNJ, excluding the inconsistency of the sources at the two sites. The seasons were classified on the basis of the running average of the temperature over five days, as suggested by Zhang (1934). As such, the seasonal aerosol number spectrum data of spring, summer, and autumn was obtained from 6–23 April 2011; 24 April–8 May 2011; and 2–24 November 2009, respectively. In the discussion of NPF events, all data

were collected at the two sites under the same synoptic system; NPF events were on the regional scale (Stanier et al., 2004a; Wu et al., 2007), and the air pollutants were on similar levels (Li et al., 2011).

### 3. Results and discussion

#### 3.1 Overview of aerosols, air pollutants, and meteorological conditions

The Air Pollution Index (API), which provides a simple and generalized method of describing air quality, is calculated from the mass concentrations of SO<sub>2</sub>, NO<sub>2</sub>, and inhalable particulate matter (PM<sub>10</sub>). Indices of <50, 50–100, and >100 correspond to excellent, good, and polluted, respectively.

Figure 2 shows the daily averaged API during the observation periods. The API in spring and autumn were relatively high with the mean value higher than 90. The index in summer was lower at 40–70 due to frequent precipitation. The dominant air pollutant in Nanjing during the observation periods was gener-

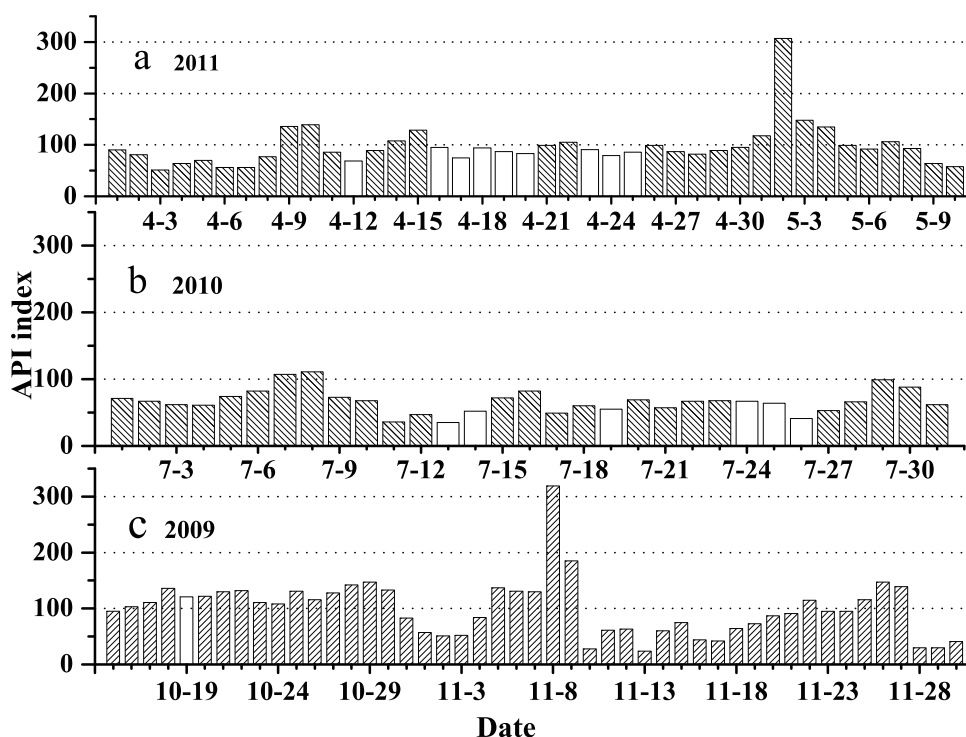


**Fig. 2.** The daily averaged API in the observation periods in Nanjing, at three periods including (a) April 2011, (b) July 2010 and (c) Oct–Nov 2009. Except API were lower than 50, the dominant pollutant was  $\text{PM}_{10}$  in all observation periods in this study. If the dominant pollutant is  $\text{PM}_{10}$ , the API of 50, 100 and 200 are correspond to  $\text{PM}_{10}$  mass concentration of  $50 \mu\text{g m}^{-3}$ ,  $150 \mu\text{g m}^{-3}$  and  $350 \mu\text{g m}^{-3}$  respectively.

ally  $\text{PM}_{10}$ . In most cases, the mass concentrations of  $\text{PM}_{10}$  were higher than  $50 \mu\text{g m}^{-3}$ , which is the typical aerosol level in urban areas (Dunn et al., 2004; Jeong et al., 2004; Wehner et al., 2004; Mönkkönen et al., 2005; Wu et al., 2007).

Figures 3–5 show time series of aerosol number, number spectrum, surface area, trace gas concentrations, and meteorological factors observed in Nanjing during the three observation periods. The total average of aerosol number concentrations was approximately  $1.8 \times 10^4 \text{ cm}^{-3}$ , which is similar to or slightly higher than that in cities such as Pittsburgh (Stanier et al., 2004a) and Leipzig (Wehner and Wiedensohler, 2003) in developed countries but significantly lower than those in megacities such as New Delhi (Mönkkönen et al., 2005), Shanghai (Gao et al., 2009), and Beijing (Hu et al., 2009) in developing countries. Ultrafine particle (0.01–0.1  $\mu\text{m}$ ) number concentrations in Nanjing accounted for 90% of the total number concentrations of particles observed, which is similar to the levels observed in the aforementioned cities. The average number concentration of accumulation mode (0.1–1.0  $\mu\text{m}$ ) particles in Nanjing was  $3.9 \times 10^3 \text{ cm}^{-3}$ , which was the same as that in Shanghai, sig-

nificantly less than those in Beijing and New Delhi, and significantly higher than those in Pittsburgh and Leipzig. The high levels of accumulation mode particles may be more common in developing countries than those in developed countries. Thus, the high number concentration of accumulation mode particles is the main reason for the poor visibility in developing countries.

The effects of wind speed/direction and precipitation scavenging on aerosols were obvious. In precipitation periods such as 10 November 2009; 20 July 2010; and 16 April 2011, the aerosol number concentrations were significantly low. The concentration was also low under strong wind speed conditions on 14 November 2009; 24 July 2010; and 22 April 2011. Under the conditions of high temperature and low relative humidity, the concentration was high. High temperature is favorable for the photochemical reactions that produce secondary aerosol particles, and low relative humidity creates adverse conditions for hygroscopic growth and coagulation of fine particles.

The prevailing wind directions in Nanjing were northerly in spring and autumn and easterly in summer. Wind speed was high in spring and weak in au-

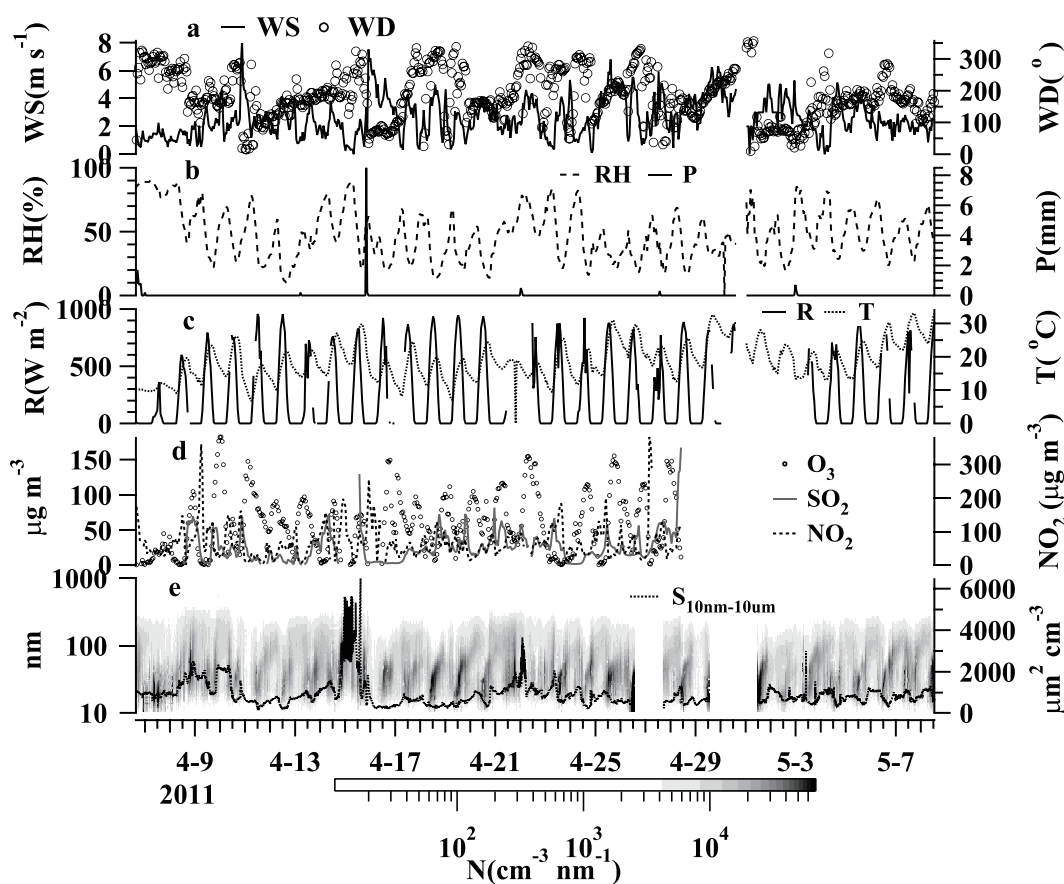


**Fig. 3.** (a, b, c) Time series of the meteorological factors, (d) trace gases concentrations, (e) aerosol surface area concentration and aerosol spectrum distribution in April of Nanjing.

tumn. In the summer monsoon season, the east winds mainly originate from the ocean and pass through the megacities of the Yangtze River Delta including Shanghai, Suzhou, and Wuxi. Sufficiently rapid air mass movement creates clean air, which is an additional reason for the low aerosol concentration in summer. In later spring and autumn, crop residual burning occurs frequently and has a high impact on the concentrations of accumulation mode particles (Yin et al., 2011).

The NPF events were easily captured in spring; nine NPF days were recorded in 21 effective observation days, which are defined as those with more than 20 h of effective data. We measured four NPF days of 19 effective observation days in summer. Although the particle number concentrations in accumulation mode were high in autumn, the number concentrations were lowest in the nuclei mode (10–30 nm); therefore, only one NPF day was captured in 35 effective observation days during that season. In section 3.3, we focus on the characteristics and meteorological conditions of these NPF events in Nanjing.

### 3.2 Seasonal and diurnal variations of aerosol concentration

#### 3.2.1 Seasonal variation of aerosol number spectrum

Figure 6 indicates that the averaged aerosol number spectra all presented two peaks in the three seasons at DTNJ. In spring and summer, two weak peaks occurred at 30 and 100 nm. The shape of the number spectrum in autumn showed distinct differences compared with those in spring and summer. In autumn, the accumulation mode particles were obviously high while the nuclei mode particles were low, with the two respective peaks occurring at 50 nm and 100–200 nm. The second peak was higher than the first. The seasonal number spectrum differences were obviously in various size ranges. For that of 10–30 nm, the number concentration ranked in the order of summer > spring > autumn; that for 30–100 nm was summer > autumn > spring. The number concentration of accumulation mode particles (100–1000 nm) ranked in the order of autumn > summer > spring, and that for coarse mode (>1 μm) particles was spring > autumn > summer.

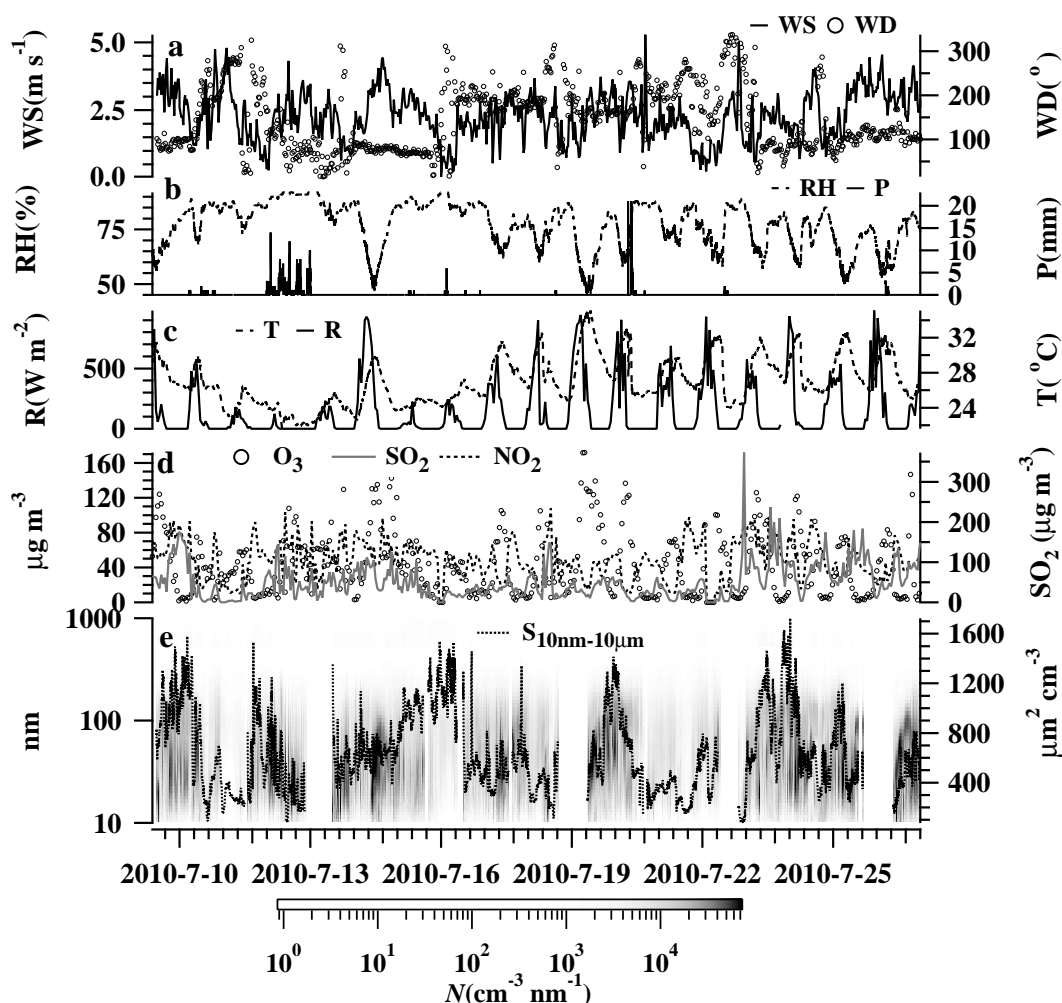


Fig. 4. The same as Fig. 3, except for Jul 2010.

Compared with spring and autumn, the number concentration of fine particles ( $<1 \mu\text{m}$ ) was generally highest, and that of coarse particles ( $>1 \mu\text{m}$ ) was extremely low in summer. Strong radiation and high temperatures in summer, which averages  $27^\circ\text{C}$ , activates atmospheric photochemical reactions to generate large amounts of secondary fine aerosol particles by the gas-particle transformation process. However, a strong scavenging effect on the coarse mode particles occurs due to frequent precipitation in that season.

The wind speed was strongest in spring at an average of  $3.3 \text{ m s}^{-1}$ . In summer and autumn, the average was  $2.3 \text{ m s}^{-1}$ . The mean relative humidity was 44% in spring, which was lower than the respective summer and autumn values of 77.4% and 64.3%. Therefore, the coarse particle number concentration was highest in spring due to the dry air and strong wind speed, which may have led to high contributions from soil and dust aerosols in local and long-range transport. The high number concentration of

the accumulation mode particles in autumn may relate to the aging and accumulating processes in the lasting air pollution events under stable weather conditions in that season. Hu et al. (2009) observed that the accumulation mode particles continuously increase under heavy pollution conditions. A pollution day is defined as that with an API of greater than 100. In our study, nine pollution days of long durations were recorded in autumn, five were recorded in spring, and only two were recorded in summer. In addition, the air quality in Nanjing was directly affected by the crop residual open burning in the harvest season (Nanjing EPA; <http://www.njhb.gov.cn/>). For example, on 8 November 2009, the heaviest air pollution of the year with API of 319 was recorded in Nanjing due to crop residual open burning (Yin et al., 2011). Such burning of agriculture biomass could release large amounts of accumulation mode particles (Li et al., 2008), which is one of the reasons attributed to the high number concentration of accumulation mode particles in autumn.

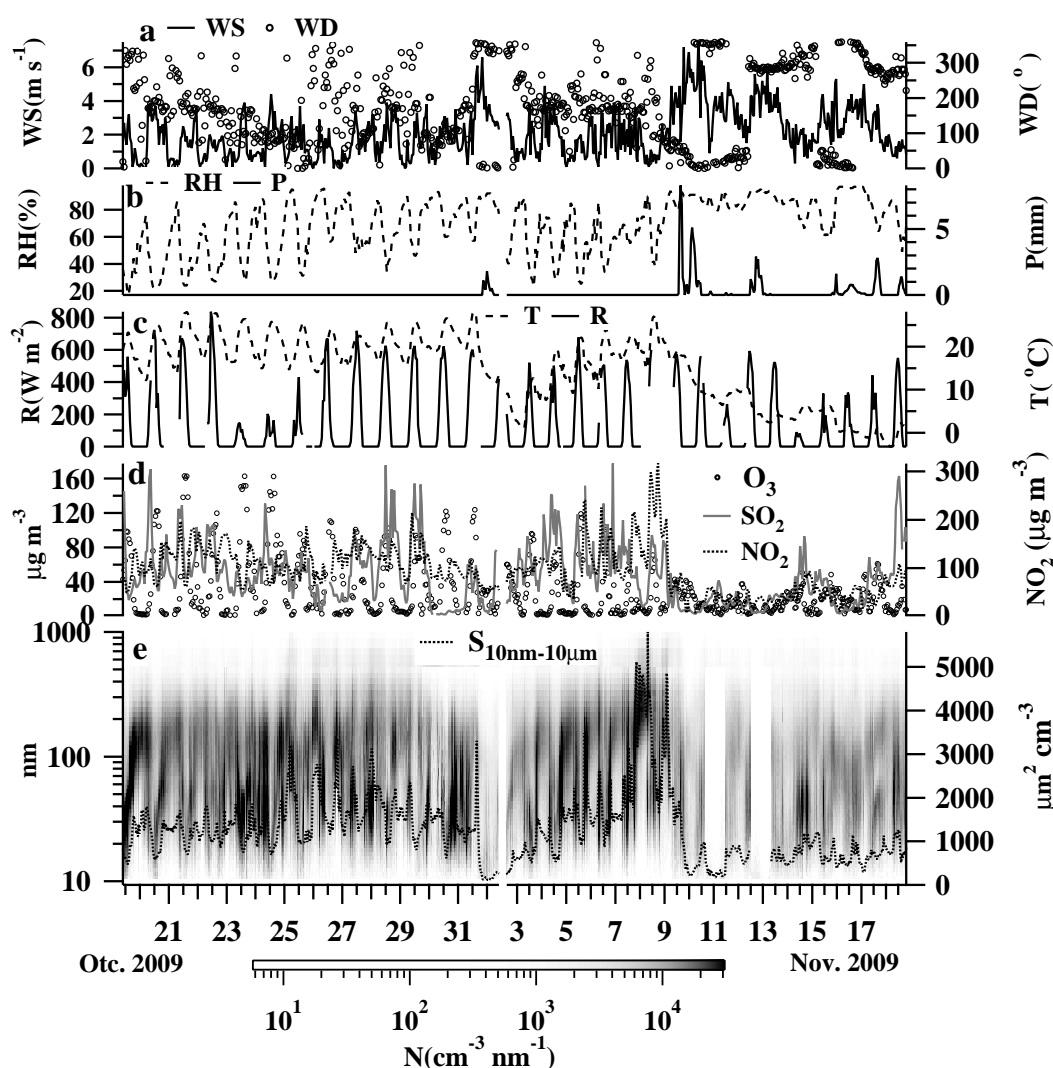


Fig. 5. The same as Fig. 3, except for 19 Oct–18 Nov 2009.

### 3.2.2 Seasonal diurnal variations of aerosol number concentration

Figure 7a showed three peaks for the averaged diurnal variations of the total aerosol number concentration in all observation seasons. The first peak and third peak were at 0800–0900 LST and 1800–2000 LST, respectively, which is mainly attributed to the influence of traffic emissions in rush hours. The construction of inversion at night and its disappearance in the morning could explain the third peak at night, which was higher than the first peak in the morning in all seasons. The second peak occurred at 1100–1400 LST and was not obvious in autumn. The highest second peak in summer was due to the secondary aerosols generated from strong photochemical reactions, and the relative lag of the second peak in spring is attributed to weak photochemical reactions.

Figures 7b–d clearly indicate the diurnal varia-

tion features of particles in various modes and seasons, which implicates the relationships of the particle sources. Particularly in summer, the nuclei mode particles (10–30 nm) peaked at noon, with the highest level at  $1.4 \times 10^4 \text{ cm}^{-3}$ . This result is attributed to previously mentioned photochemical activities. Except the peak at noon in summer, the Aiken mode particles presented similar diurnal variation features in the total number concentration, with two distinct peaks appearing at the rush hours. The noon peak of the Aiken mode particles in summer and spring occurred 1–2 h after that for the nuclei mode particles. In autumn, the nuclei mode particles were lowest and did not show obvious diurnal variation. However, the accumulation mode particle (100 nm–1  $\mu\text{m}$ ) levels in autumn were significantly high and showed two peaks in the morning and evening. In autumn, the persistent air pollution events were frequent. The accom-

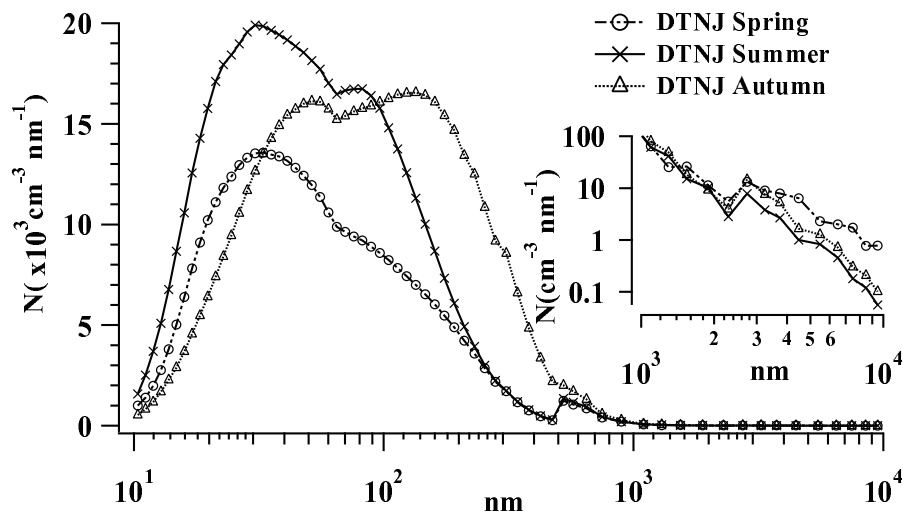


**Fig. 6.** Seasonal variations of average aerosol number spectrum at DTNJ in Nanjing. The season classification was based on the five days temperature running average, suggested by Zhang (1934).

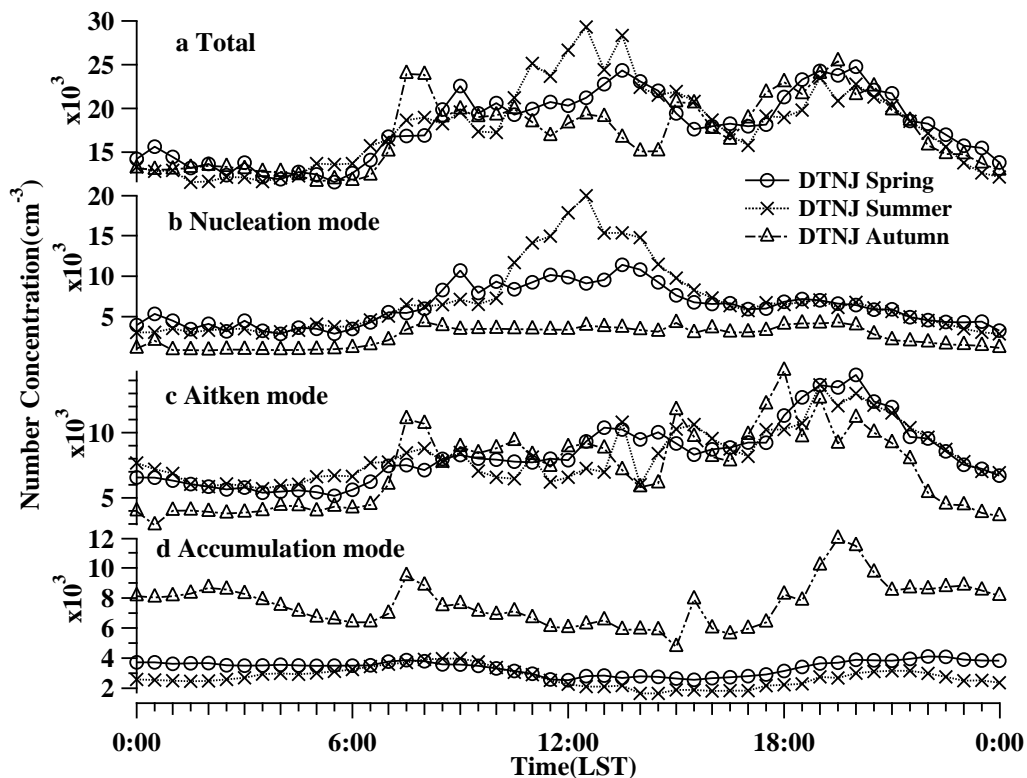


**Fig. 7.** The diurnal variations of aerosol number concentration in different seasons at DTNJ of Nanjing. The season classification was the same as Fig. 6.



panying coagulation and condensation processes were favorable for decreasing the amount of particles in the nuclei mode and increasing those in the accumulation mode. As previously mentioned, crop residual open burning also contributed significantly to the amount of particles in the accumulation mode. Therefore, the heavy air pollution in autumn led to high particle concentration in the accumulation mode and low particle concentration in the nuclei mode.

### 3.3 New particle formation event analysis

The following NPF characteristics have been reported in previous research: (1) The particle number in the new nuclei mode of 10–30 nm appears, persists for several hours, and increases at a rate of a few nanometers per hour (10 nm is the lowest detection limit of WPS in this study); and (2) such a sharp increase in nuclei mode particles is not marked by a simultaneous increase of pollutant emissions from traffic or industrial sources, including SO<sub>2</sub>, CO, NO<sub>x</sub>, and surface area concentration of aerosols (Kulmala et al., 2004a, b; Dal Maso et al., 2005; Wu et al., 2007; Gao et al., 2009; Hu et al., 2009; Shen et al., 2011).

On the basis of these criteria, the characteristics and related meteorological conditions of NPF observed at the two sites in Nanjing in October 2009, July 2010, and April 2011 were analyzed. As shown in Figs. 3–5, high-frequency NPF events were captured in spring and summer; only one occurred in autumn.

The beginning and end times of the NPF are generally estimated by the increasing and decreasing times of nuclei mode aerosol number concentration (Birmili et al., 2003; Gao et al., 2009). In this study, the points

at which the number concentration in the size of 10–30 nm increased or decreased to the 1/e of its maximum concentration were defined as the beginning or end time of the NPF, respectively. All of the NPF events occurred in the daytime, indicating that the formation of new particles is closely related to photochemical processes. Tables 2 and 3 summarize the duration times of the NPF, changes in nuclei mode particles, total surface area of particles, and trace gas concentrations that occurred during the NPF processes.

Table 2 indicates that the 10–30 nm number concentration was significantly high with a value of more than 10<sup>4</sup> cm<sup>-3</sup> in summer when NPF events occurred. However, the concentration was relatively lower in spring. As previously discussed, strong solar radiation and high temperatures in summer favor NPF. In the size range of 10–30 nm, the background number concentrations were approximately 6000 cm<sup>-3</sup> and 5000 cm<sup>-3</sup> in summer and spring, respectively. The total surface area concentration was 420–639 μm<sup>2</sup> cm<sup>-3</sup> in summer when the NPF events occurred, with values usually higher than 500 μm<sup>2</sup> cm<sup>-3</sup>, and 279–430 μm<sup>2</sup> cm<sup>-3</sup> in spring, with values usually less than 400 μm<sup>2</sup> cm<sup>-3</sup>.

The growth rate (GR) of NPF events was calculated according to that reported by Dal Maso et al. (2005) and Hu et al. (2009):

$$\text{GR} = \frac{\Delta D_m}{\Delta t}, \quad (1)$$

where  $D_m$  is the geometric mean diameter of nuclei mode particles and  $\Delta t$  is time interval. The unit of GR is nm h<sup>-1</sup>.

Table 2 indicates that the GR was highest in sum-

**Table 2.** Summaries of the beginning time, end time, number, surface area and trace gas concentrations in NPF events in the observation periods of Nanjing.

Date (month-day)	$N_{10\sim 30\text{nm}}$ (cm <sup>-3</sup> )	$S_{10\text{nm}\sim 10\mu\text{m}}$ (μm <sup>2</sup> cm <sup>-3</sup> )	GR (nm h <sup>-1</sup> )	$dN/dt$ (cm <sup>-3</sup> h <sup>-1</sup> )	O <sub>3</sub> (μg m <sup>-3</sup> )	SO <sub>2</sub> (μg m <sup>-3</sup> )	NO <sub>2</sub> (μg m <sup>-3</sup> )
13 Jul	19390	556	15.2	25387	64.74	57.97	53.44
14 Jul	13174	639	13.5	25684	97.32	75.10	55.72
19 Jul	11557	544	12.1	10136	121.86	21.64	28.42
24 Jul	14518	572	10.5	13106	27.26	95.01	70.65
25 Jul	15961	420	14.3	13378	31.99	50.95	42.72
26 Jul	17194	308	12.9	13730	45.55	27.34	24.48
12 Apr	9603	279	7.7	7404	90.72	5.73	13.88
16 Apr	10304	312	8.3	6053	80.78	19.47	36.01
17 Apr	10560	647	6.8	9684	78.16	52.90	71.84
18 Apr	16145	356	7.5	12712	82.35	31.59	29.24
19 Apr	13581	430	6.9	7147	107.68	42.37	39.12
20 Apr	12786	529	12.1	6775	135.39	31.85	42.70
23 Apr	15350	601	7.8	12414	138.06	26.53	30.53
24 Apr	8802	395	7.5	8027	100.35	28.35	26.25
25 Apr	13130	796	7.1	9851	121.75	50.87	44.58
19 Oct	12335	602	7.3	11321	75.99	54.46	65.07

**Table 3.** The meteorological factors in the NPF events of Nanjing.

Date (month-day)	Start time (LST)	End time (LST)	Temp. (°C)	RH (%)	Solar (W m <sup>-2</sup> )	WS (m s <sup>-1</sup> )	WD (°)
13 Jul	1200	1551	24.5	83	124.2	2.2	58
14 Jul	0850	1803	27.9	60	538.5	3.6	77
19 Jul	0840	1732	32.7	55	605.1	2.8	162
24 Jul	0809	1030	29.5	72	685.8	3.1	83
25 Jul	0920	1223	29.4	68	406	3.2	102
26 Jul	0910	1400	30.1	61	635.6	3.0	134
12 Apr	1000	1530	19.2	14.4	510	3.8	149
16 Apr	1040	1600	17.9	25.2	394	6.1	77
17 Apr	0930	1530	19.3	31	688.5	3.6	204
18 Apr	0805	1540	17.0	23.8	520	4.2	291
19 Apr	0927	1542	16.6	28.4	572	2.8	230
20 Apr	0940	1700	21.6	23	687.7	3.4	161
23 Apr	1110	1640	23.0	28	606.3	3.3	267
24 Apr	1130	1600	19.7	31	586.2	2.0	248
25 Apr	1000	1540	25.8	32	725	5.5	194
19 Oct	0950	1530	21.5	25.9	421	2.2	228

mer with values of 10–16 nm h<sup>-1</sup>. In spring, the rate was lower with values of 6.8–8.3 nm h<sup>-1</sup>. The GR was 7.3 nm h<sup>-1</sup> in the sole autumn NPF event. In comparison, Kulmala et al. (2004a, b) summarized the new particle typical GR as 1–20 nm h<sup>-1</sup> in the boundary layer. Gao et al. (2009) observed a GR of approximately 6–7 nm h<sup>-1</sup> in Shanghai. Wu et al. (2007) and Hu et al. (2009) observed a GR of approximately 8–12 nm h<sup>-1</sup> in summer in Beijing. Stanier et al. (2004b) evaluated the regional nucleation events by using the number concentration formation rate (cm<sup>-3</sup> h<sup>-1</sup>) in nuclei mode particles. Similarly, we calculated the  $dN_{30}/dt$  in Table 2, where  $N_{30}$  is the particle number concentration within 10–30 nm. Stronger regional nucleation events were captured in summer than those in spring and autumn.

Table 3 shows meteorological factors that occurred during the NPF events. The NPF events in summer were under the conditions of prevailing east winds (2–4 m s<sup>-1</sup>) with high temperature (25°C–33°C), strong solar radiation (400–700 W m<sup>-2</sup>), and high relative humidity (50%–70%), which was higher than that in Beijing (10%–40%). The sources of air mass can influence the chemical compositions and number spectrum of particles. The back trajectories in Fig. 1b indicate that the air masses were mainly from east and southeast in July in the NPF periods. The spring NPF events occurred with high temperature (16°C–20°C), low relative humidity (14%–30%), strong solar radiation (400–600 W m<sup>-2</sup>), and moderate wind speed (3–6 m s<sup>-1</sup>) with no dominant directions. Generally, the air masses originating from marine regions in summer and spring were relatively clean, which enabled easy observation of the NPF events. It should be noted that the

API remained below 100 in all NPF days. The lowest value at 52 occurred on 14 July, for which an ideal NPF was captured (Fig. 8c). We have determined that the heavy air pollution in autumn led to the high particle concentration in the accumulation mode. The process of coagulation on the pre-existing particles was the dominant sink of the nuclei mode particles. As such, coagulation on the accumulation mode particles could have led difficulty in capturing NPF events during that season.

Figure 8c shows two ideal NPF events on 14 July 2010, and 10 April 2011. In the two cases, the 10–30 nm number concentration began to increase at 0900 on 14 July and at 0830 LST 19 April. However, 30–100 nm number concentration and total surface area of the aerosols began to increase on 0930 LST 14 July and on 0920 LST 19 April, 30–90 min after the nuclei mode particle increase (Fig. 8b). This delay could be attributed to the rapid growth of the new particles at the rate of approximately 10 nm h<sup>-1</sup>. As indicated in Table 2, the GR was 13.5 nm h<sup>-1</sup> on 14 July and 6.9 nm h<sup>-1</sup> on 19 April.

The mass concentrations of O<sub>3</sub> were generally higher than 60 μg m<sup>-3</sup> in all seasons during NPF events, except for 24–26 July. The level was 97 μg m<sup>-3</sup> on 14 July, 121 μg m<sup>-3</sup> on 19 July, and 75 μg m<sup>-3</sup> on 19 October. All exceeded 80 μg m<sup>-3</sup> in all NPF events in spring, implying a relationship between NPF events and photochemical reactions.

The O<sub>3</sub> concentrations corresponded well with the number concentrations in NPF events shown in Fig. 8a; no significant correlations were observed with NO<sub>2</sub> and SO<sub>2</sub>. We divided the NPF period into two phases. The first is the developing phase, represent-

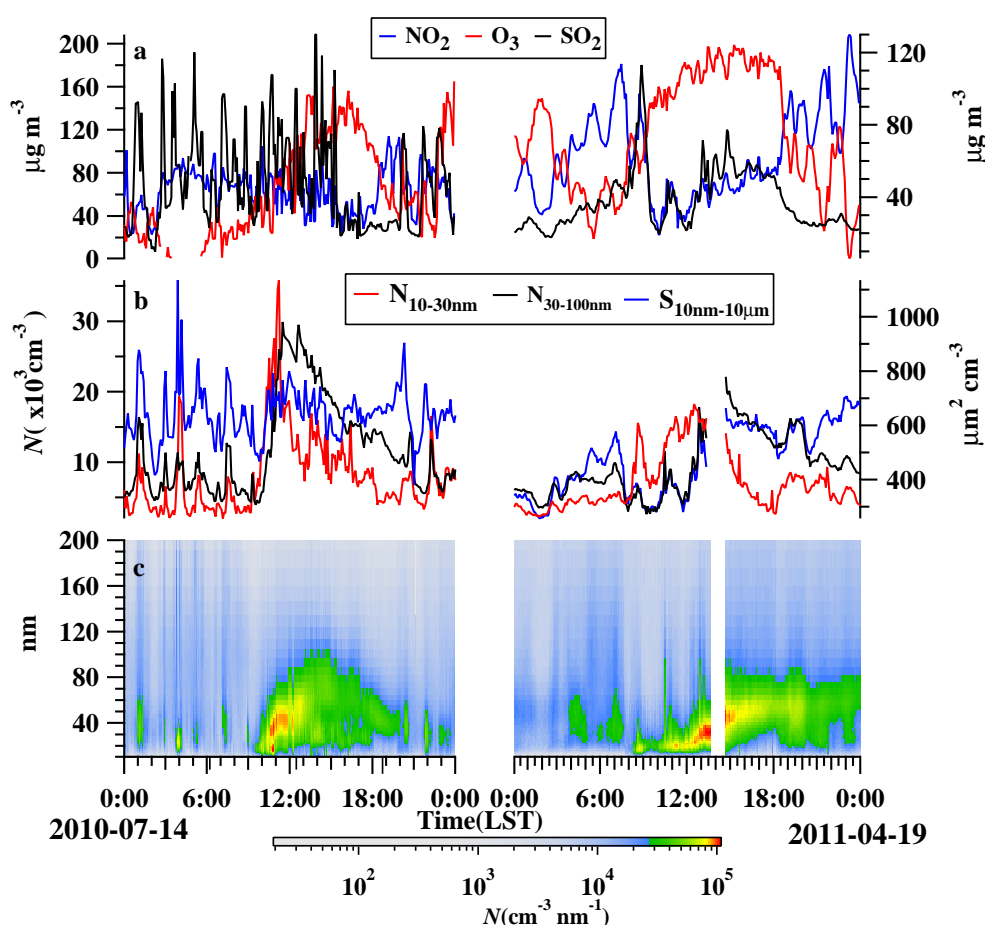


Fig. 8. (a) Time series of trace gases concentrations, (b) aerosol number and surface area concentration and (c) aerosol spectrum distribution in the two typical NPF events in Nanjing.

ing the beginning of NPF to the point at which the number concentration of 10–30 nm particles reaches its maximum value. The second is the aging phase, representing the point at which the number concentration of 10–30 nm particles reaches its maximum value to the end of NPF event. Positive correlation was detected in the developing phase of NPF with correlation coefficients of 0.6–0.9, which are high values for the spring season. The high correlation between  $\text{O}_3$  and new particles in the developing phase of NPF indicated that the gas-to-particle photochemical transformation process is a direct reason for NPF. Due to the product of UV radiation and  $\text{SO}_2$ , which can be used as a surrogate parameter for  $\text{H}_2\text{SO}_4$  production (Petaja et al., 2009), extended positive correlation of  $\text{UV} \times \text{SO}_2$  to nuclei particles was detected in NPF events in summer, further suggesting the photochemical effects on NPF. However,  $\text{SO}_2$  and  $\text{NO}_2$ , as the precursor gases and factors in photochemistry, did not show significant correlation with NPF.  $\text{H}_2\text{SO}_4$  has been generally identified as an important atmospheric nucleating

species; other precursor gases implicated in NPF include  $\text{NH}_3$ , organic acids, and ion clusters (Zhang et al., 2004; Wang et al., 2010), which increases considerable uncertainty of NPF in urban air (Guo et al., 2012). In this study, measurements of such compounds were limited, which created difficulties in determining the complex relationships between NPF and aerosol precursor gases. Therefore, further investigations of chemical components of ultrafine particles and their precursor inorganic/organic gases are required.

#### 4. Summaries

The results of this study are summarized in the following points:

(1) Distinct size differences were apparent in the seasonal variations of aerosol number concentrations in Nanjing. The number concentrations of particles in the nuclei mode (10–30 nm), Aitken mode (30–100 nm), accumulation mode (100–1000 nm) and coarse mode ( $>1 \mu\text{m}$ ) varied in the order of summer  $>$  spring

> autumn, summer > autumn > spring, autumn > summer > spring, and spring > autumn > summer, respectively. In summer, the highest concentrations of nuclei mode particles were related to photochemical processes. In autumn, the highest concentrations of accumulation mode particles may be related to the accumulation processes in the persistent air pollution, and the lowest concentrations of nuclei mode particles could be attributed to the coagulation sink under high levels of accumulation mode particles.

(2) The diurnal variations of aerosol spectrum show three peaks in all the three seasons occurring at 0800–0900, 1200–1400, and 1900–2000 CST, which corresponded to two rush hours and the noon period of photochemistry.

(3) In comparison with cities in northern China, the NPF in summer in Nanjing developed under conditions of high relative humidity (50%–70%), high temperature (25°C–33°C), strong solar radiation (400–700 W m<sup>-2</sup>), and moderate wind speed (2–4 m s<sup>-1</sup>) with air masses originating mainly from marine regions. In spring, the NPF were generally accompanied by low temperature (16°C–20°C), low relative humidity (14%–30%), and strong solar radiation (400–600 W m<sup>-2</sup>). However, under severe air pollution conditions, NPF was seldom detected in autumn. The GR were highest in summer with values of 10–16 nm h<sup>-1</sup>; those recorded in spring were 5.9–7.5 nm h<sup>-1</sup>.

(4) In NPF periods, positive correlations between number concentrations of 10–30 nm aerosols and O<sub>3</sub> were detected, particularly in spring, indicating that photochemical reactions are one of the chief reasons for NPF.

**Acknowledgements.** This research was funded by the Special Fund for Public Welfare Industrial (Meteorology) Research of China (Grant No. GYHY201206021-04), National Natural Science Foundation of China (Grant Nos. 41030962 and 41005089), Jiangsu “333” Program, Jiangsu “Qinglan” program, Graduate Cultivation Innovative Project of Jiangsu province (Grant No. CXZZ11-0616), and the Priority Academic Program Development (PAPD) of Jiangsu Higher Education Institutions.

## REFERENCES

- Birmili, W., H. Berresheim, C. Plass-Dülmer, T. Elste, S. Gilge, A. Wiedensohler, and U. Uhrner, 2003: The Hohenpeissenberg aerosol formation experiment (HAFEX): A long-term study including size-resolved aerosol, H<sub>2</sub>SO<sub>4</sub>, OH and monoterpenes measurements. *Atmos. Chem. Phys.*, **3**, 361–376.
- Boy, M., and Coauthors, 2005: Sulphuric acid closure and contribution to nucleation mode particle growth. *Atmos. Chem. Phys.*, **5**, 863–878.
- Castro, A., E. Alonso-Blanco, M. González-Colino, A. I. Calvo, M. Fernández-Raga, and R. Fraile, 2010: Aerosol size distribution in precipitation events in León, Spain. *Atmospheric Research*, **96**, 421–435.
- Dal Maso, M., M. Kulmala, I. Riipinen, R. Wagner, T. Hussein, P. P. Aalto, and K. E. J. Lehtinen, 2005: Formation and growth of fresh atmospheric aerosols: eight years of aerosol size distribution data from SMEAR II, Hyytiälä, Finland. *Boreal Environment Research*, **10**(5), 323–336.
- Donaldson, K., D. Brown, A. Clouter, R. Duffin, W. MacNee, L. Renwick, L. Tran, and V. Stone, 2002: The pulmonary toxicology of ultrafine Pparticles. *Journal of Aerosol Medicine*, **15**(2), 213–220.
- Dunn, M. J., J. L. Jimenez, D. Baumgardner, T. Castro, P. H. McMurry, and J. N. Smith, 2004: Measurements of Mexico city nanoparticle size distributions: Observations of new particle formation and growth. *Geophys. Res. Lett.*, **31**(10), L10102, doi: 10.1029/2004GL01948.
- Gao, J., T. Wang, X. Zhou, W. Wu, and W. Wang, 2009: Measurement of aerosol number size distributions in the Yangtze River Delta in China: Formation and growth of particles under polluted conditions. *Atmos. Environ.*, **43**(4), 829–836.
- Gong, Y. G., M. Hu, W. W. Song, J. Gao, F. Liu, and Y. H. Zhang, 2011: Atmospheric nucleation rate at Xinken site in the Pearl River Delta of China. *Environmental Science*, **32**(4), 930–935. (in Chinese)
- Guo, H., D. W. Wang, K. Cheung, Z. H. Ling, C. K. Chan, and X. H. Yao, 2012: Atmospheric chemistry and physics observation of aerosol size distribution and new particle formation at a mountain site in subtropical Hong Kong. *Atmos. Chem. Phys.*, **12**, 9923–9939, doi: 10.5194/acp-12-9923-2012
- Holmes, N. S., 2007: A review of particle formation events and growth in the atmosphere in the various environments and discussion of mechanistic implications. *Atmos. Environ.*, **41**(10), 2183–2201.
- Horvath, H., M. Kasaharat, and P. Pesava, 1996: The size distribution and composition of the atmospheric aerosol at a rural and nearby urban location. *Journal of Aerosol Science*, **3**, 417–435.
- Hu, M., L. Y. He, X. F. Huang, and Z. J. Wu, 2009. *Atmospheric Fine Particles and the Physical and Chemical Characteristics of Ultrafine Particles, Origin and Formation Mechanism in Beijing*. Science Press, Beijing, 241–277.
- Hussein, T., and Coauthors, 2009: Time span and spatial scale of regional new particle formation events over Finland and southern Sweden. *Atmos. Chem. Phys.*, **9**, 4699–4716.
- Jeong, C. H., P. K. Hopke, D. Chalupa, and M. Utell, 2004: Characteristics of Nucleation and Growth Events of Ultrafine Particles Measured in Rochester, NY. *Environmental science & technology*, **38**(7), 933–1940.
- Jung, C. H., and Y. P. Kim, 2006: Numerical estimation of the effects of condensation and coagulation on vis-

- ibility using the moment method. *Journal of Aerosol Science*, **37**(2), 143–161.
- Kuang, C., P. H. McMurry, and A. V. McCormick, 2009: Determination of cloud condensation nuclei production from measured new particle formation events. *Geophys. Res. Lett.*, **36**(9), doi: 10.1029/2009GL037584.
- Kulmala, M., H. Vehkamäki, T. Petäjä, M. Dal Maso, A. Lauri, V.-M. Kerminen, W. Birmili, and P. H. McMurry, 2004a: Formation and growth rates of ultrafine atmospheric particles: A review of observations. *Aerosol Science*, **35**(2), 143–176.
- Kulmala, M., and Coauthors, 2004b: Initial steps of aerosol growth. *Atmos. Chem. Phys.*, **4**, 2553–2560.
- Li, J. X., Y. Zhao, L. J. Li, X. G. Yang, H. J. Li, X. Dong, and Y. T. Yang, 2008: Characterization of ambient air pollution in Beijing caused by agricultural burning. *Acta Scientiae Circumstantiae*, **28**(9), 1904–1909. (in Chinese)
- Li, W., L. Shao, Z. Wang, R. Shen, S. Yang, and U. Tang, 2010: Size, composition, and mixing state of individual aerosol particles in a South China coastal city. *Journal of Environmental Sciences*, **22**(4), 561–569.
- Li, Y. Q., B. Zhu, and J. L. An, 2011: A comparative of long-path and traditional point atmospheric pollutants monitoring technique. *Journal of Nanjing University of Information Science and Technology: Natural Science Edition*, **3**(2), 128–136.
- Mäkelä, J. M., and Coauthors, 1997: Observations of ultrafine particle formation and growth in boreal forest. *Geophys. Res. Lett.*, **24**(10), 1219–1222.
- McMurry, P. H., and K. S. Woo, 2002: Size distributions of 3–100nm urban Atlanta aerosols: Measurement and observations. *Journal of Aerosol Medicine*, **15**(2), 169–178.
- Mönkkönen, P., I. K. Koponen, K. E. J. Lehtinen, K. Hämeri, R. Uma, and M. Kulmala, 2005: Measurements in a highly polluted Asian mega city: Observations of aerosol number size distribution, modal parameters and nucleation events. *Atmos. Chem. Phys.*, **5**, 57–66.
- Natusch, D. F. S., and J. R. Wallace, 1974, Urban aerosol toxicity: The influence of particle size. *Science*, **186**(4165), 695–699.
- Odum, J. R., T. P. W. Jungkamp, R. J. Griffin, R. C. Flagan, and J. H. Seinfeld, 1997: The atmospheric aerosol-forming potential of whole gasoline vapor. *Science*, **276**(5309), 96–99.
- Opsis, A. B., 2003: Quality assurance and quality control using Opsis analysers for air quality monitoring (Version 1.4). Opsis A B, Sweden, 9–69.
- Petäjä, T., and Coauthors, 2009, Sulfuric acid and OH concentrations in a boreal forest site. *Atmos. Chem. Phys.*, **9**, 7435–7448, doi: 10.5194/acp-9-7435-2009
- Putaud, J. P., R. V. Dingenen, and A. Alastuey, 2010: A European aerosol phenomenology-3: Physical and chemical characteristics of particulate matter from 60 rural, urban, and kerbside sites across. *Europe Atmospheric Environment*, **44**, 1308–1320.
- Qian, L., Y. Yin, Y. Q. Tong, W. W. Wang, and Y. X. Wei, 2008: Characteristics of size distributions of atmospheric fine particles in the north suburban area of Nanjing. *China Environmental Science*, **28**(1), 18–22. (in Chinese)
- Riipinen, I., and Coauthors, 2007: Connections between atmospheric sulfuric acid and new particle formation during QUEST III-IV campaigns in Heidelberg and Hyytiälä. *Atmos. Chem. Phys.*, **7**, 1899–1914.
- Shen, X. J., and Coauthors, 2011: First long-term study of particle number size distributions and new particle formation events of regional aerosol in the North China Plain. *Atmos. Chem. Phys.*, **11**, 1565–1580.
- Stanier, C. O., A. Y. Khlystov, and S. N. Pandis, 2004a: Ambient aerosol size distributions and number concentrations measured during the Pittsburgh air quality study (PAQS). *Atmos. Environ.*, **38**(20), 3275–3284.
- Stanier, C. O., A. Y. Khlystov, and S. N. Pandis, 2004b: Nucleation events during the Pittsburgh air quality study: Description and relation to key meteorological, gas phase, and aerosol parameters. *Aerosol Science and Technology*, **38**(S1), 253–264.
- Wang, L., A. F. Khalizov, J. Zheng, W. Xu, Y. Ma, V. Lal, and R. Zhang, 2010: Atmospheric nanoparticles formed from heterogeneous reactions of organics. *Nature Geoscience*, **3**, 238–242, doi: 10.1038/ngeo778.
- Wehner, B., W. Birmili, and T. Gnauk, 2002: Particle number size distributions in a street canyon and their transformation into the urban air background: Measurements and a simple model study. *Atmos. Environ.*, **36**, 2215–2223.
- Wehner, B., and A. Wiedensohler, 2003: Long term measurements of submicrometer urban aerosols: Statistical analysis for correlations with meteorological conditions and trace gases. *Atmos. Chem. Phys.*, **3**, 867–879.
- Wehner, B., A. Wiedensohler, T. M. Tuch, Z. J. Wu, M. Hu, J. Slanina, and C. S. Kiang, 2004: Variability of the aerosol number size distribution in Beijing, China: New particle formation, dust storms, and high continental background. *Geophys. Res. Lett.*, **31**(22), doi: 10.1029/2004GL021596.
- Wu, Z. J., and Coauthors, 2007: New particle formation in Beijing, China: Statistical analysis of a 1-year data set. *J. Geophys. Res.*, **112**(D9), doi: 10.1029/2006JD007406.
- Yin, C., B. Zhu, Y. C. Cao, J. F. Su, X. Y. Wang, and H. Wang, 2011: The origin of crop residue burning impact on air quality of Nanjing. *China Environmental Science*, **31**(2), 207–213. (in Chinese)
- Zhang, B. K., 1934: The Duration of Four Seasons in China. *Acta Geographica Sinica*, **1**(1), 29–74. (in Chinese)
- Zhang, R., I. Suh, J. Zhao, D. Zhang, E. C. Fortner, X. Tie, L. T. Molina, and M. J. Molina, 2004: Atmospheric new particle formation enhanced by organic acids. *Science*, **304**(5676), 1487–1490.